ISSN: 2096-3246
Volume 55, Issue 09, September, 2023

Effect of Upward Inclination Angle on Flow Energy Loss in Symmetrical and Asymmetrical Venturi Meters for Single-Phase Incompressible Isothermal Low Reynolds Number Turbulent Flows

Keith Wells[1], Ahmad Sharifian[1]

School of Engineering, University of Southern Queensland, Darling Heights QLD 4350, Australia[1]

Keywords:
Symmetrical Venturi meters, permanent pressure loss, low Reynolds number turbulent flow, inclination angle.

ABSTRACT

The Venturi flow meter provides various measurement options in piped systems for liquids, gas, steam and slurries. Measuring fluid flow with a Venturi flow meter results in permanent pressure loss due to the friction on the walls of the meter, cone angles and geometry transition points. The ISO-5167 standard specifies the geometry and method of use for Venturi meters installed in a horizontal orientation for unidirectional flows with Reynolds numbers higher than 200,000. This research aims to investigate and compare the performance of a symmetrical Venturi meter with an ISO-5167 meter in terms of permanent pressure loss at upward inclination angles for flows with a Reynolds number of ≈34,000. The key findings from the research indicate that both symmetrical and ISO-5167 Venturi meters can be installed vertically to save room, and this does not increase the permanent pressure losses for single-phase incompressible isothermal low Reynolds number turbulent flows. Furthermore, the results indicate that the permanent pressure loss in a vertical orientation may decrease slightly, a trend particularly noticeable in the ISO-5167 Venturi meter.

1. INTRODUCTION

Two established methods exist for reducing fluid pressures without requiring any moving parts. The first is the split chimney mechanism [1], [2], which uses hot surfaces and buoyancy effects to induce a swirling flow. Extensive research [2] has been conducted on this approach, which has applications in generating fire whirls [1], [2], diluting exhaust gas [3], [4], and improving the efficiency of Savonius turbines [5- 9]. However, this mechanism has a limited application since it only functions in a vertical orientation. The second mechanism uses the Venturi effect. The Venturi effect has a wide range of industrial applications, which include flow measurement, spray nozzles and wind tunnels [10- 13], ventilation [14], air-conditioning [15], refrigeration [16], [17], heat transfer systems [18], automotive carburettor systems and rocket propulsion [19]. The medical industry also utilizes the Venturi effect, notably in measuring arterial blood flow [20] and in technologies related to artificial respiration [21]. This study focuses only on the

applications of Venturi meters for flow measurement.

Flow measurement of industrial fluids in pipelines must be simple, precise, low energy loss, and cost-effective [22], [23]. The Venturi flow meter has many advantages over other types of flow meters. The meter has no moving parts, which reduces the required maintenance, and it is not vulnerable to over-speeding. The Venturi meter is suitable for liquids, gases and slurry mixtures because there are no small orifices or vanes to become blocked. The Venturi meter can be used for high-pressure and temperature applications and operate in both flow directions [24].

The ISO-5167 standard [25] provides guidelines for manufacturing and installing Venturi flow meters. The standard specifies the geometry and operational methodology for single-phase horizontal fluid flow with Reynolds numbers of 200,000 to 2,000,000. The ISO-5167 standard suggests an absolute roughness criterion of less than 10^{-4} of the throat diameter.

There are some applications not covered by the standard, such as low Reynolds number flows (< 200,000) (some medical applications), bi-directional flow (artificial respiration instruments), non-horizontal operations such as mobile applications (carburettor) and where the space is limited (inclined or vertical installation). This research aims to investigate the performance of classical asymmetrical Venturi meters for an incompressible isothermal single-phase low Reynolds number turbulent flow and compare its performance in terms of permanent pressure loss with that of symmetrical Venturi meters at upward inclination angles.

To the best of the authors' knowledge, based on an extensive literature review, there are no previous studies on the impact of the inclination angle on Venturi performance for single-phase flow. Two articles evaluate such an impact, but these papers discuss the inclination effect for two-phase flow. The experimental study of [26] on the impact of the inclination angle for the two-phase flow of R134a found that the lowest permanent pressure loss occurs during vertical upward flow through the Venturi. A numerical study on the impact of the inclination angle on the two-phase flow of oil and water, conducted by [27], found that the permanent pressure loss increases as the mounting angle increases. Although it is impossible to compare their results because the flow parameters were different, their studies present the possible impact of the inclination angle on the performance of Venturi meters in the case of single-phase flow.

The Venturi meter can cause considerable energy loss during its life span. Prior to installing the Venturi meter, a tube matching the length, diameter (D), and surface roughness of the Venturi meter is installed in the system, and the inlet pressure ($P_{1,TUBE}$) and outlet pressure ($P_{3,TUBE}$) are measured. The equivalent length tube is replaced with the Venturi meter, and the pressures at the inlet ($P_{1,VEN}$), throat ($P_{2,VEN}$) and outlet ($P_{3,VEN}$) are measured. The difference between the two pressure losses, as shown in Equation 1, indicates the permanent pressure loss ($\Delta P_{Permanent}$) due to the Venturi meter.

$$\Delta P_{Permanent} = (P_{1,VEN} - P_{3,VEN}) - (P_{1,TUBE} - P_{3,TUBE}) \quad (1)$$

A crucial metric of flow meter performance is the coefficient of discharge (Cd), which is the ratio of the actual volume flow rate to the theoretical volume flow rate, as shown in Equation 2.

$$Q = C_d \sqrt{\frac{2(P_{1,VEN} - P_{2,VEN})}{\rho}} \frac{A_D}{\sqrt{\left(\frac{A_D}{A_d}\right)^2 - 1}} \quad (2)$$

Q is the volume flow rate, ρ is the fluid density, and A_D and A_d are the cross-sectional areas of the Venturi entry and throat, respectively.

Venturi flow meters' measurement accuracy and sensitivity improve when ($P_{1,VEN} - P_{2,VEN}$) increases. This difference can be increased by reducing the throat size, resulting in higher permanent pressure losses. A more accurate and balanced measure of Venturi performance is the relative pressure loss coefficient (ζ), shown in Equation 3.

$$\zeta = \frac{(P_{1,VEN} - P_{3,VEN}) - (P_{1,TUBE} - P_{3,TUBE})}{P_{1,VEN} - P_{2,VEN}} = \frac{\Delta P_{Permanent}}{P_{1,VEN} - P_{2,VEN}} \quad (3)$$

In the design of a Venturi meter, it is desirable to have the lowest ζ, which requires a small value in the numerator and a large value in the dominator of Equation 3.

2. Literature review

Many studies use the ISO-5167 standard for guidance to help calibrate methodologies [28], [29]. ISO-5167 characterizes the specification of Venturi meters for unidirectional flow in the Reynolds number range of 200,000 to 2,000,000 and the pipe diameters ranging from 50 mm to 1200 mm. The ISO-5167 standard recommends a convergent cone angle of 21° ±1° and a divergent cone angle of between 7° to 15°. The standard also recommends detailed guidelines on the Venturi construction.

A computational study by [30] indicates that when the roughness of the Venturi wall increases from 0 μm to 1000 μm, there is a decrease of 2.7% in the Cd for incompressible flow. They increased the convergent and/or divergent cone angle beyond the specifications of ISO-5167, reduced the Cd for incompressible flow and found that the variation in Cd was more sensitive to changes in the divergent cone angle than the convergent cone angle. The findings indicate that the value of ζ is sensitive to changes in the ratio of the throat diameter to the inlet diameter (β-ratio), as demonstrated by the slight decrease of 0.5% in Cd. The research of [31] demonstrates that the accelerated flow in the convergent section of a Venturi reduces the thickness of the boundary layer, and the fluid flow becomes closer to the surface of the meter, keeping the flow stable and relatively free of turbulence. This concept is consistent with the research of [32], who found that negative pressure gradients suppress flow separations. Since the convergent section is not prone to flow separation, the convergent angle can be relatively large.

The divergent section of a Venturi meter has the most effect on energy loss [33]. When fluid flow experiences an increasing pressure gradient, the fluid outside the boundary layer has enough momentum to overcome the pressure trying to push it against it. However, the fluid momentum within the boundary layer is small and can reverse when overcoming the pressure increases in the divergent section, causing flow separation [31].

Research by [34] suggests that for divergent cone angles less than 7°, flow separation will not occur. A study by [35] indicates that angles greater than 15° can result in flow separation for the Reynolds number range of 1.5×10^5 to 2×10^6. An explanation for discrepancies in the literature on divergent cone angles is

presented in the research of [33], who suggest that flow separation also depends on the Reynolds number. Although there is an array of literature on the classical Venturi, there is no literature concerning symmetrical Venturi meters. Symmetrical geometry enables bidirectional flow measurement, potentially extending the applications of the meter.

3. Methodology

This study aims to address the gaps in existing research using computational and empirical methodologies, focusing on single-phase, isothermal, incompressible turbulent flows with low Reynolds numbers. The research evaluates the impact of upward inclination angles of 0°, 30°, 45°, 60°, and 90° on the permanent pressure loss for a symmetric and an asymmetric Venturi meter.

3.1 Experimental Approach

3.1.1 Experimental setup

The experimental setup is shown in Figure 1. The setup includes a pump, pump controller, two types of Venturi meters, PVC pipes and tubes, accumulator, drain, recycle tank, three pressure gauges and a testing apparatus to mount the Venturi meters at different inclination angles.

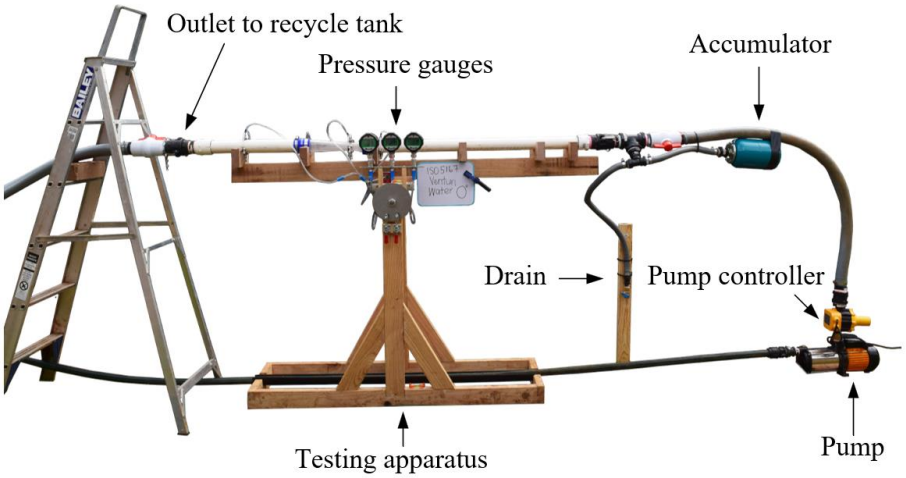

Figure 1. Experimental setup at an inclination angle of 0°.

A pump with a flow capacity of 150 L/min delivered the pressurized water. The suction pipe of the pump was attached to the bottom of a 1000 L recycle tank.

The pivot system enabled the mounting of Venturi meters at different angles. Two flange bearings were incorporated into the pivot system design so that the inclination angle could be easily adjusted, as shown in Figure 2a.

ISSN: 2096-3246
Volume 55, Issue 09, September, 2023

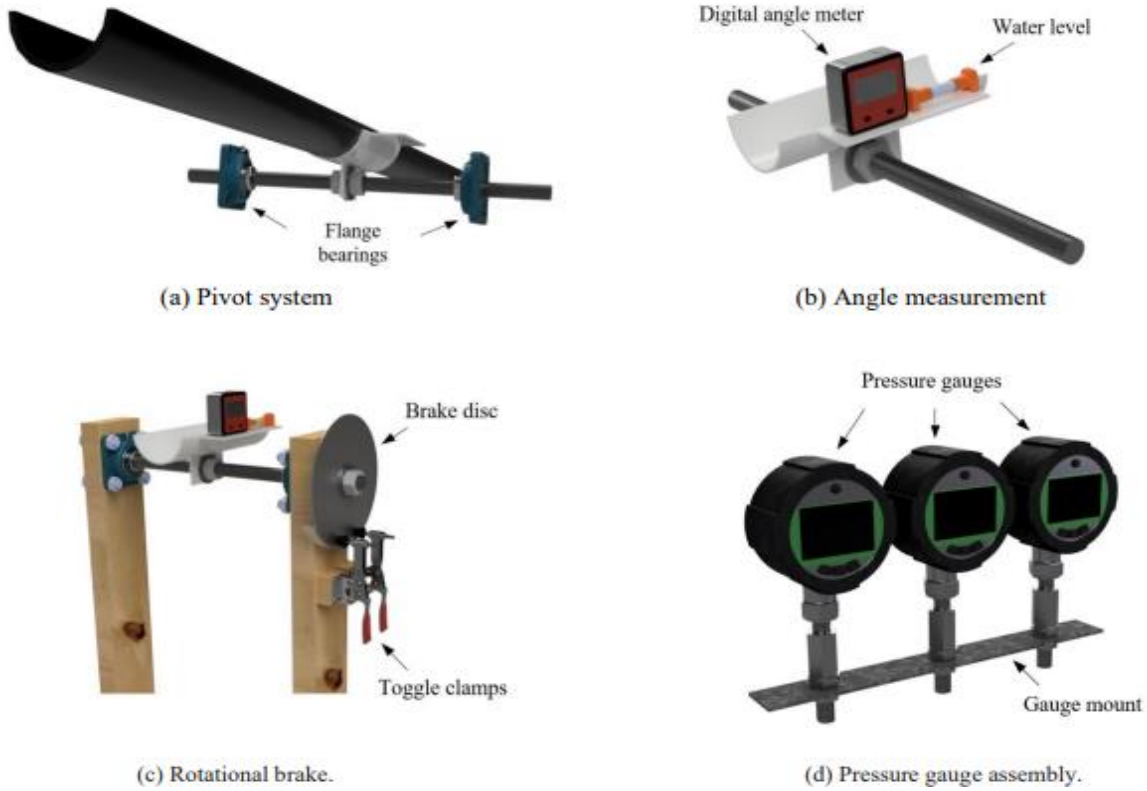

Figure 2. Main components of the testing apparatus.

A digital angle meter was fitted to the pivot system (see Figure 2b) so the Venturi meters could be aligned with the mounting angles. A rotational brake was designed for the mounting system to lock the orientation to the required angle, as shown in Figure 2c. Three pressure gauges were mounted to the testing apparatus. The gauges were positioned near each other to be viewed simultaneously (Figure 2d). The complete testing apparatus is shown in Figure 3.

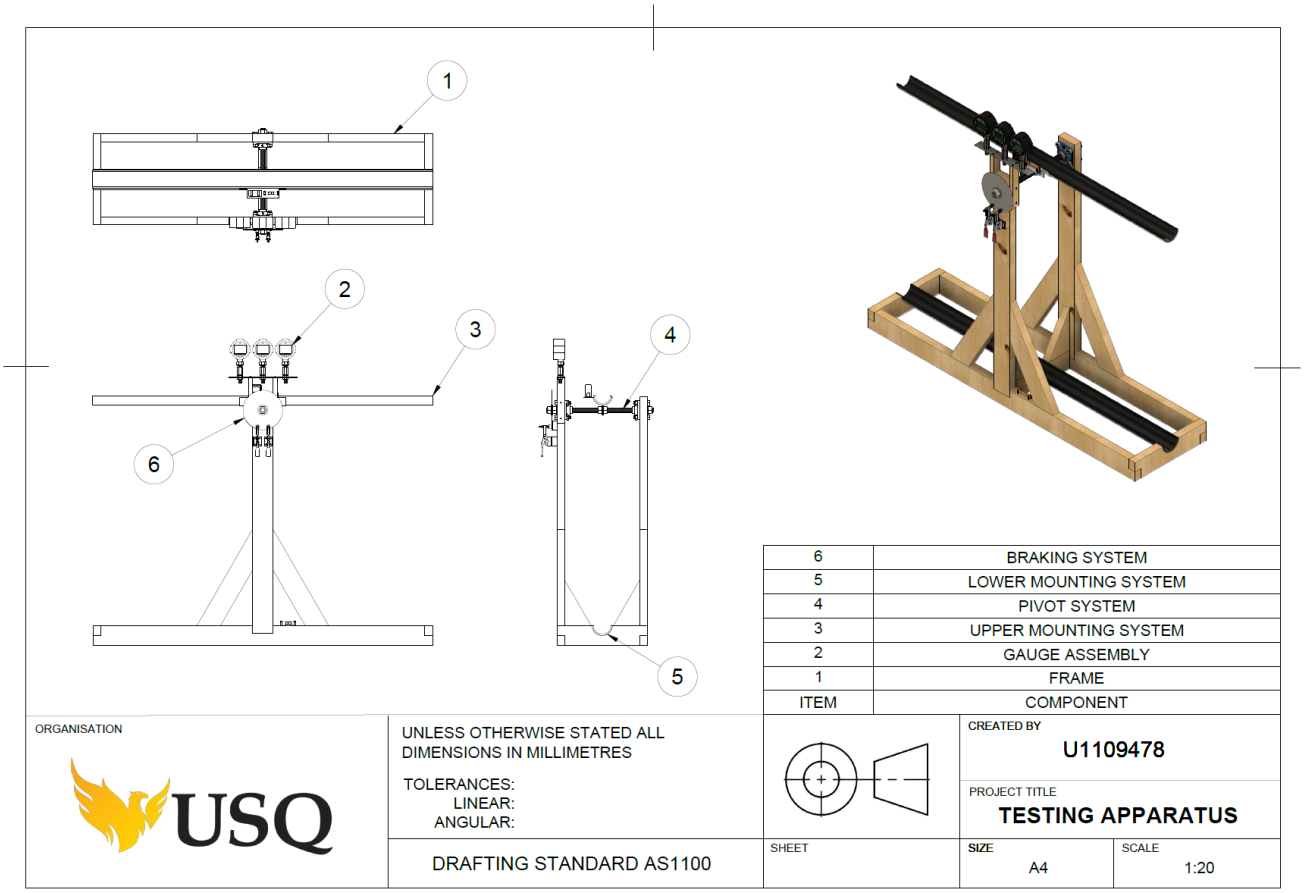

Figure 3. Testing apparatus.

3.1.2 Venturi Meters

Ten Venturi meters were designed and printed. The first Venturi meter matched the specifications prescribed in the ISO-5167 standard, and other Venturi meters had symmetrical cone angles. Post-processing finishing techniques were applied to the internal surface of the Venturi meters to ensure a roughness value of 2 µm was achieved, which aligned with the prescribed specifications in the ISO-5167 standard. Finally, all Venturis were tested, and the one with the lowest permanent pressure loss (SVD7) at the horizontal mounting orientation was selected for this study. Table 1 presents the geometry of both meters.

Table 1. Venturi flow meter designs.

Venturi	β	Throat Length= Throat diameter (mm)	Convergent/divergent cone angle	Venturi Length (mm)
ISO5167	0.55	27.5	21°/7°	302.14
SVD7	0.70	35	10°/10°	236.46

The ISO-5167 standard specifies that the pressure tappings for the inlet and outlet should be located at least 1D (inlet diameter) upstream of the inlet flange and 6D downstream of the outlet flange, respectively. The printed Venturi meters only include the throat pressure tapping points. The standard also specifies a

minimum of four pressure tappings for the throat manufactured from separate pipes, joined together by a triple tee arrangement with a fourth cross piece providing the connection for the pressure gauge [25]. Stainless tubing was inserted into the four pressure-tapping holes in the Venturi meter, and the manifold was fitted to each meter, as shown in Figure 4.

(a) SVD7 Venturi meter. (b) ISO-5167 Venturi meter.

Figure 4. Venturi meters.

3.1.3 Experimental Uncertainties

Each experiment was performed twenty times, and the average temperature of experiments was 18℃± 1℃, which led to an uncertainty of ±2.6% in calculating the viscosity and the Reynolds number. The water level in the 1000 L recycle tank was maintained at approximately 500 L. A stopwatch and a 35 L measurement tank (Figure 5) were used to measure the flow rate of each experiment. No measurable differences in the flow rate were observed in any of the experiments. The operator response time depends on their attention level, which varies with age and other factors. The response time of the operator is estimated to be an average value of ±0.5s [36], [37]. Therefore, as the flow rate was 1.33 L/s, an uncertainty of ±2% in measuring the flow rate can be expected. The digital angle meter was factory calibrated to ±0.2°, which was regularly checked at 0° and 90° using a water level. An additional water level was added to the frame of the testing apparatus to ensure that testing occurred on level ground. Considering the short length of the Venturi meters, this caused a minor uncertainty of up to 0.1 Pa.

Based on the specifications of the manufacturer, the precision of the pressure gauges was ±0.02% on a full scale of 30 kPa, leading to an uncertainty of ±6 Pa. However, the pressure gauges had a resolution of 10 Pa. Therefore, the uncertainty of the measured pressure was ±10 Pa, the uncertainty of the measured pressure change in the tube and Venturi was ±20 Pa, the uncertainty of permanent pressure loss was ±40 Pa, and the uncertainty of comparing pressure losses of the two Venturi meters was ±80 Pa.

Figure 5. Flow measurement system.

3.2 Computational Approach

3.2.1 Details of Computational Modelling

CFD simulations were conducted on the ISO-5167 and SVD7 meters at 0°, 30°, 45°¸60° and 90° of upward inclination, using water as the fluid. Since the flow parameters in ANSYS Fluent can be easily adjusted, the experimental fluid supply determined the flow conditions for the research. The Venturi meters and equivalent-length PVC tubes were generated with axisymmetric modelling. The cone angles, inclination angles, section lengths and diameters were set as parameters. The boundary conditions were set to mass flow rate at the inlet, the outlet was a pressure outlet, and the walls were no slip. A structured quadrilateral mesh was chosen for the Venturi simulations, as recommended by [38].

A structured quadrilateral mesh was chosen for the Venturi simulations because it provided accurate results at higher-order schemes and improved numerical stability [38]. The height of the first mesh cell at the boundary of the domain was calculated by applying the theory of the 'law of the wall'. This process of determining y^+ is explained in research by [39]. The research of [40] recommended a y^+ value of less than five, with the ideal value being one for SST k-ω models. The y^+ value of one was also suggested as a target in the CFD studies of [29], [30]. Applying the flow conditions and the recommended y^+ value gave an initial mesh layer height of ≈0.004 mm. The mesh height in the boundary layer was refined to provide a gradual growth progression into the primary mesh of the Venturi. Conducting a 2D axisymmetric simulation provided an analysis with higher stability and faster convergence.

The mesh generated for the mesh independence study is shown in Figure 6. The mesh was created for a symmetrical Venturi meter with 10° cone angles and an internal pipe diameter of 50 mm. The highest skewness value for the Venturi mesh was ≈0.057 (Figures 6a and 6b), and the minimum orthogonal quality was ≈0.994 (Figures 6c and 6d), which meant that the geometric structure of the mesh was excellent [41].

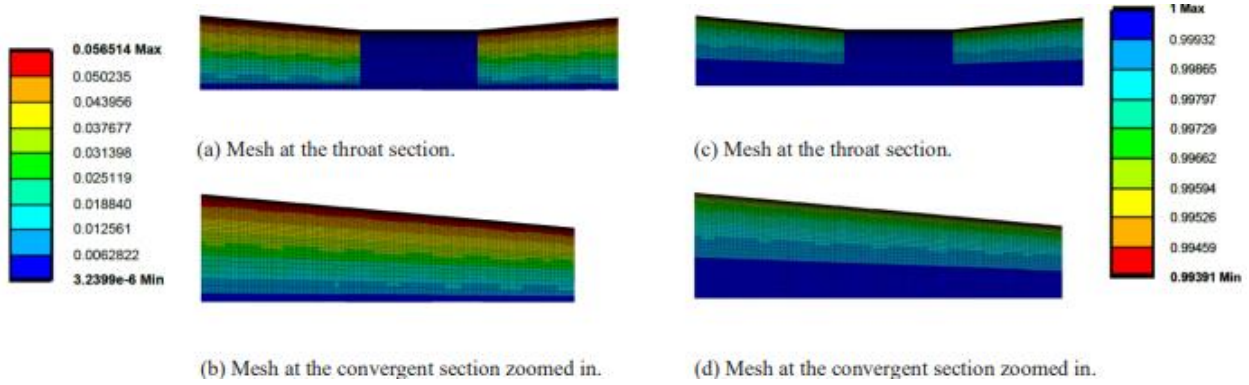

Figure 6. Skewness and orthogonal quality of the symmetrical Venturi mesh.

The exact Reynolds number for the experimentation was determined to be 33754, indicating that the flow conditions of the Venturi meter were mildly turbulent. The Shear Stress Transport (SST) k-omega (k-ω) model was selected for the CFD simulations as recommended by [38].

The ANSYS Fluent solver selected for the simulation used a coupled algorithm. Although the coupled solver uses more computational resources and experiences a slower convergence than the segregated approach, the result is more accurate [42]. The simulation applied a pseudo-transient method, which meant that the simulation was not entirely dependent on time. The pseudo-transient method can provide faster convergence and typically results in more realistic results [40]. The residual values for the continuity equation, velocity components and turbulence were less than 10^{-8}. A second-order scheme was employed to

solve the governing equations.

A mesh independence study was conducted to identify the minimum resolution required for the CFD solution to be independent of the mesh element size. The mesh independence study used an approximated mass flow rate of 1.411 kgs^{-1} and a velocity value of 0.720 ms^{-1} as the input variables. Eighteen structured Venturi meshes were generated using mesh element sizes ranging from 0.5 mm to 9.5 mm. The output parameters evaluated in the mesh independence study were velocity, the velocity increase factor, pressure drop and the conservation of mass. The results from the mesh independence study are shown in Figures 7a, b, c, and d.

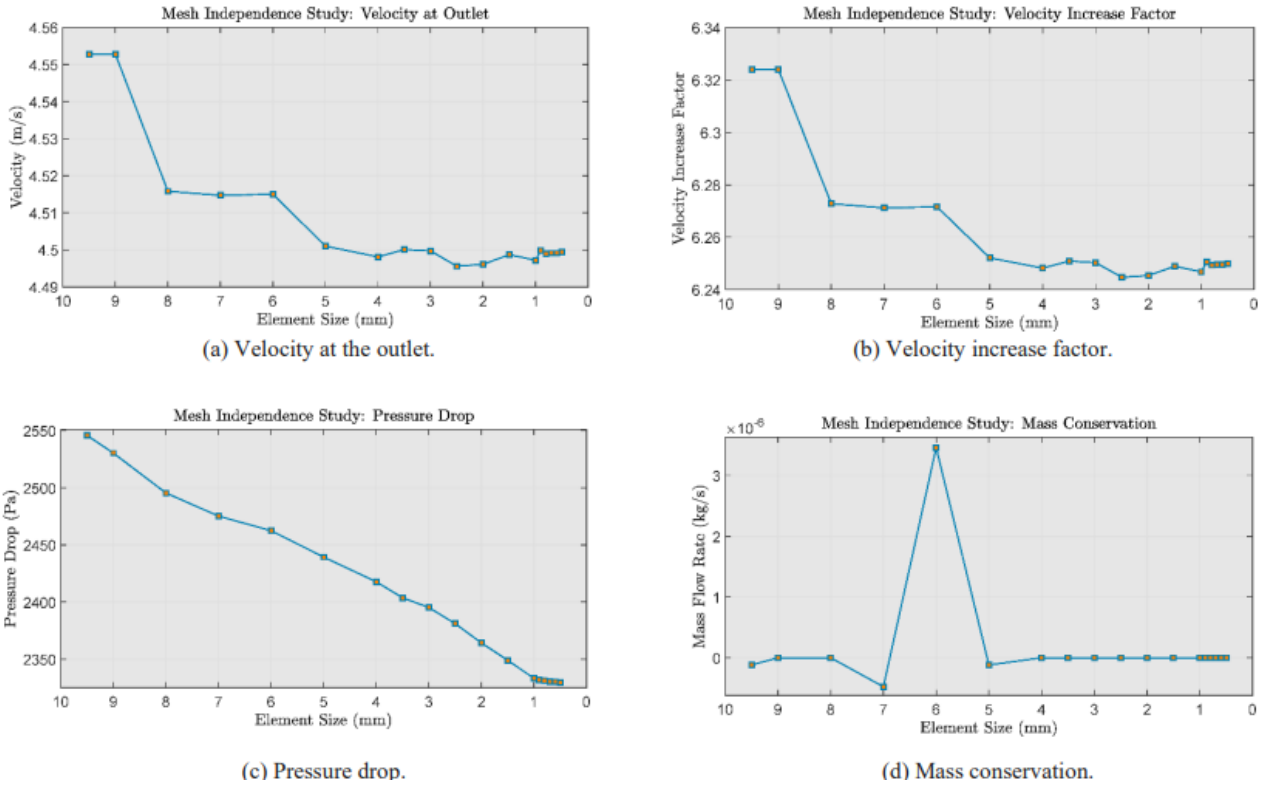

(a) Velocity at the outlet.

(b) Velocity increase factor.

(c) Pressure drop.

(d) Mass conservation.

Figure 7. Mesh independence study.

The mesh independence study showed that the values for velocity, the velocity increase factor, pressure drop and the conservation of mass stabilized when the mesh element size was approximately 1 mm. The number of mesh elements at 1 mm was 39300 with 40137 mesh nodes.

3.2.2 Validation of Computational Results

The pressure tapping points were not included in the CFD analysis, which did not allow the extent of the static hole error to be measured. Not including the static hole in the simulation is expected to create a minor disparity between the simulation analysis and the experimental results. Although the research of [43] recommends a method to account for the static hole error, it is only an approximation.

The methodology for the CFD analysis was validated with the experimental results for Cd and ζ using ISO-5167. The results show a difference of 2.18% in the Cd between the CFD simulation and the experimental results and 10.41% for the ζ, demonstrating relatively close alignment, as shown in Table 2.

Table 2. Validation of methodology for Venturi ISO-5167 at the horizontal mounting orientation

(Re = 33754, Q = 0.00133 m^3s^{-1}, e = 2 µm).

	CFD	Experimental	% Difference
Cd	0.96899	0.94808	2.18
ζ	0.11396	0.12648	10.41

The Cd values from the CFD simulations and experimental analysis of the ISO-5167 Venturi closely align with the results of [44], who reported a value of 0.97 for Cd at a Reynolds number of 33754.

4. Results

The velocity contour plots at an inclination angle of 0° for the ISO-5167 and SVD7 Venturi meters are presented in Figure 8. The figures show that the change of velocity for the ISO-5167 meter is greater than that of the SVD7 Venturi, as the β value (0.55) is less than the SVD7 Venturi (0.7).

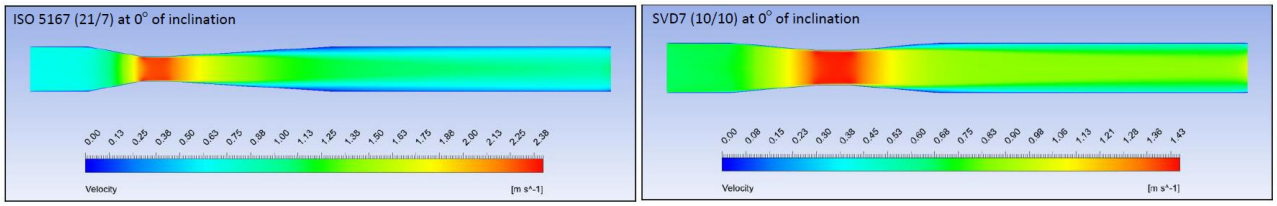

Figure 8. Velocity contour plots for the ISO-5167 and SVD7 water analysis at an inclination angle of 0° (Re = 33754, Q = 0.00133 m^3s^{-1}).

The eddy viscosity contours for the ISO-5167 and the SVD7 for a 0° inclination angle (Figure 9) demonstrate that the level of turbulence in the divergent section is higher for the ISO-5167 than the SVD7 even though the ISO-5167 meter has a smaller divergent cone angle. The higher turbulence for the ISO-5167 Venturi could be expected due to its lower β value and larger convergent cone angle. The interesting finding is that the flow at the outlet pressure tapping point of the ISO-5167 Venturi is more developed than that of the SVD7 Venturi.

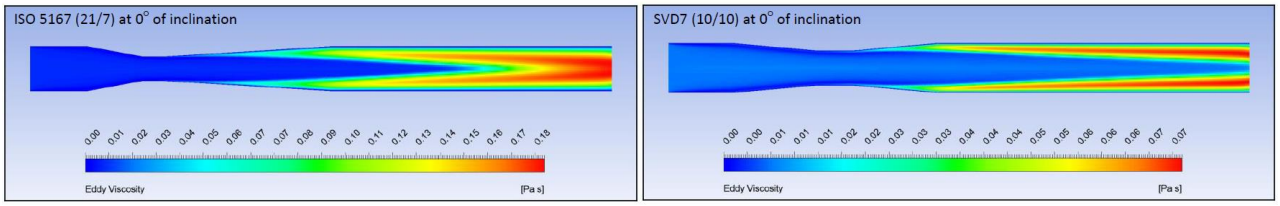

Figure 9. Turbulence contour plots for the ISO-5167 and SVD7 water analysis at an inclination angle of 0° (Re = 33754, Q = 0.00133 m^3s^{-1}).

The results for the computational static pressure analysis at inclination angles of 0° and 90° for the two Venturi meters are presented in Figure 10. The figure shows that at an inclination angle of 0º, the minimum pressure point is at the throat of the two Venturi meters, as expected. However, as the inclination angle increases, the minimum pressure point moves to the Venturi outlet. As such, the pressure at the divergent section of the two Venturi meters does not increase, which is expected to hinder the separation of the boundary layer from the wall.

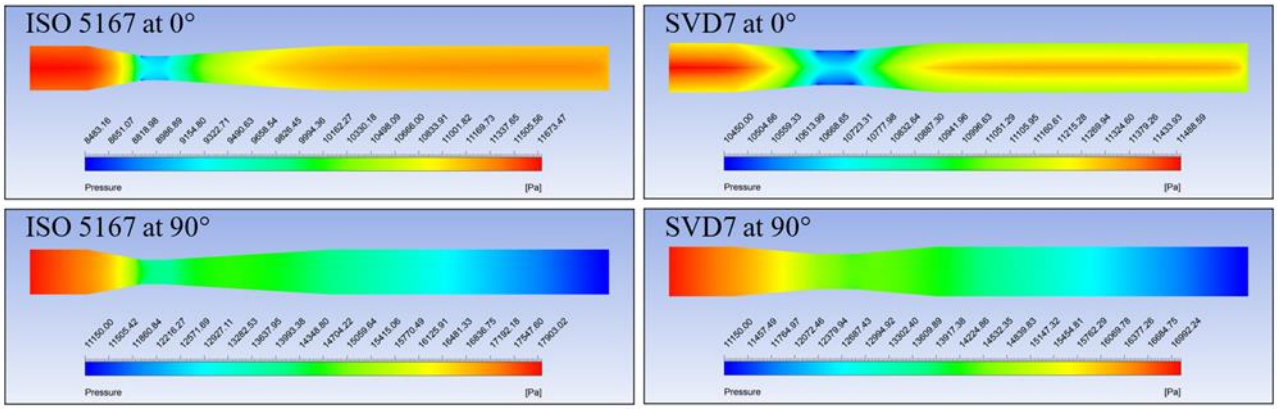

Figure 10. Pressure contour plots for the ISO-5167 and SVD7 water analysis for horizontal and vertical mounting orientations (Re = 33754, Q = 0.00133 m^3s^{-1}).

The centreline pressures of the ISO-5167 and SVD7 Venturi meters and equivalent length PVC tubes from the CFD simulations and experimental analysis are presented in Table 3. The permanent pressure loss was calculated using Equation 2. The experimental data in the table are the average values of twenty experiments.

The first part of Table 3 presents the computational results for the ISO-5167 Venturi at different inclination angles. The results show that the inclination angle has no impact on the permanent pressure loss, and the slight change of permanent pressure loss (0.01 kPa) is within the uncertainties of the study. The computational results for SVD7 Venturi (β=0.7) demonstrate lower permanent pressure losses than the ISO-5167 Venturi (β=0.55), which was expected due to a higher β value. The maximum fluctuation of the permanent pressure loss is 0.04 kPa, which is within the uncertainties of this study. However, the computational results show that the permanent pressure loss for both Venturi meters tends to increase slightly between horizontal and vertical orientations.

The experimental results follow the pattern in the simulation. The ISO-5167 Venturi demonstrates a higher permanent pressure loss than the SVD7 Venturi meter. The minimum and maximum permanent pressure losses are 0.20 kPa and 0.34 kPa, respectively. The difference between the two permanent pressure losses is 0.14 kPa, which is above the maximum pressure measurement uncertainty. The minimum and maximum permanent pressure losses of the SVD7 Venturi are 0.07 kPa and 0.16 kPa, respectively. The difference between the two permanent pressure losses is slightly above the uncertainty of the pressure measurements. This difference might be due to the distinct impact of the pressure-tapping holes at the various inclination angles, which were not modelled in the computational work. Similar to the computational results, the experimental results for both Venturi meters demonstrate an increase in permanent pressure losses between the horizontal and vertical orientations.

Table 3. Centreline pressure values for CFD and experimental water analysis (Re = 33754, Q = 0.00133 m^3s^{-1}).

Venturi	Inclination	$P_{1,VEN}$ (kPa)	$P_{3,VEN}$ (kPa)	$P_{1,TUBE}$ (kPa)	$P_{3,TUBE}$ (kPa)	$\Delta P_{pernamanent}$ (kPa)
ISO-5167 (CFD)	0°	11.70	11.30	11.43	11.30	0.27
	30°	14.85	11.32	14.58	11.33	0.28
	45°	16.14	11.32	15.87	11.32	0.27
	60°	17.11	11.30	16.84	11.30	0.27

	90°	17.87	11.25	17.60	11.25	0.27
SVD7 (CFD)	**0°**	11.49	11.34	11.42	11.33	0.06
	30°	14.34	11.28	14.26	11.28	0.08
	45°	15.49	11.27	15.42	11.27	0.07
	60°	16.37	11.26	16.26	11.25	0.10
	90°	17.04	11.21	16.97	11.21	0.07
ISO-5167 (Experimental)	**0°**	11.79	11.34	11.47	11.34	0.32
	30°	14.99	11.36	14.66	11.37	0.34
	45°	16.12	11.31	15.86	11.35	0.30
	60°	17.16	11.31	16.95	11.32	0.22
	90°	17.87	11.24	17.72	11.29	0.20
SVD7 (Experimental)	**0°**	11.60	11.34	11.47	11.30	0.09
	30°	14.52	11.32	14.32	11.25	0.13
	45°	15.55	11.24	15.43	11.28	0.16
	60°	16.37	11.24	16.29	11.26	0.10
	90°	17.20	11.28	17.04	11.19	0.07

5. Discussion

The computational and experimental results of this study demonstrate that the permanent pressure loss of Venturi meters with a β value of 0.55 is higher compared to Venturi meters with β values of 0.7 for low Reynolds number turbulent flow. This finding is consistent with previous studies at higher Reynolds number ranges. The computational results demonstrate stable and relatively low turbulence at the convergent section of the Venturi for low Reynolds number turbulent flow, which is consistent with the study of [31], [32].

The computational results of the study indicate that the flow is not fully developed at the distance of 6D downstream of the symmetrical Venturi meters. This finding does not cause any issues in practice, as there is no need to have pressure tapping points at the outlet. The Venturi meters used for volume flow rate measurement only require pressure tapping points at the inlet and throat.

The computational results of this research demonstrate that an increase in inclination angle does not increase the permanent pressure loss caused by both Venturi meters employed in the study. However, the experimental results suggest that both Venturi meters have a lower energy loss when mounted vertically. The decrease in permanent pressure losses was indicative for the SVD7 Venturi but conclusive for the ISO-5167 Venturi. This trend can be justified by considering that in the vertical orientation, the negative pressure gradient is expected to decrease due to the weight of the fluid. The effect is especially noticeable for the ISO-5167 Venturi due to its lower beta ratio, longer length, larger pressure gradient and higher turbulence, as shown in the divergent section of Figure 10. This finding is consistent with the results presented by [26]. The pressure tapping points that were not incorporated into the model are believed to play a significant role in the generation of turbulence. As a result, the computational findings cannot conclusively demonstrate a reduction in persistent pressure loss. This study conclusively demonstrates that by installing the Venturi in a vertical orientation, the energy losses will not increase and may even decrease for both Venturi meters. This finding holds significant implications as it extends the applicability of Venturis to situations where space is limited.

The potential reduction in energy consumption resulting from replacing an ISO-5167 Venturi meter with the SVD7 is significant and in line with the United Nations' goal of achieving net-zero emissions by 2050. The SVD7 Venturi has symmetrical geometry, meaning the energy losses are not dependent on the flow direction, while the ISO-5167 Venturi has a higher energy loss in reverse flow due to a large divergent cone angle (21º). Reversing the flow direction can reduce fluid transportation hardware, which is the case in applications such as pumped hydro energy storage systems. However, the energy savings are not only due to the operating cost. Practical applications require the consideration of the costs associated with manufacturing, installation, and service life.

This study has limitations, and additional research is required before definite recommendations can be made on some findings. Further research could be conducted in a controlled ambient temperature, using pressure gauges with a high accuracy of about 1 Pa and including downward inclination angles.

6. Conclusion

The methodology applied in the research aligned crucial parameters of the analysis with well-established international standards and published literature as part of a verification process. CFD simulations were validated with the relatively close alignment of data from the experimental analysis. The study demonstrated several conclusive results for single-phase, isothermal, incompressible, low Reynolds number turbulent flow (Re≈34,000) as follows:

1. The β-ratio has the highest effect on the permanent pressure loss for low Reynolds number turbulent flows.
2. The computational work demonstrates that for a relatively high divergent cone angle of 10º, the flow is not fully developed at the distance of 6D downstream of the symmetrical Venturi. However, this does create any issue for Venturi meters, as there is no need to have any pressure tappings at the outlet.
3. Both symmetrical and ISO-5167 Venturi meters can be installed vertically for applications with space limitations. The computational and experimental results of the study demonstrate that when these Venturi meters are operated in a vertical orientation, the energy loss will not increase.
4. The study also suggests that energy loss may decrease in upward vertical orientation due to a reduced likelihood of boundary layer separation from the walls. This finding is significant because it enables the fabrication of shorter asymmetric Venturi meters with larger divergent cone angles for vertical installation.

7. References

[1] Al-Atresh, S.R., Sharifian, A.S. and Wandel, A.P., 2014. The effect of the width and number of gaps on the characteristics of swirl flow induced natually inside split channel using hot air inlet. International Journal of Materials, Mechanics and Manufacturing, 2(4), pp.339-344.

[2] Al-Atresh, R.S., Sharifian, S.A. and Al-Faruk, A., 2012, January. The effect of inlet velocity and temperature on the strength of the swirling induced by a split channel: a CFD approach. In Proceedings of the 18th Australasian Fluid Mechanics Conference (AFMC 2012). University of Southern Queensland.

[3] Al Atresh, S.R., Sharifian, S.A. and Kueger, B., 2012, March. Using a split chimney for dilution of exhaust pollution: A CFD approach. In International Conference on Fluid Dynamics and Thermodynamics Technologies: FDTT (pp. 156-161).

[4] Sharifian, A. and Hashempour, J., 2012, January. Dilution of toxic gases and smoke emissions from residential chimneys using a low-cost cap. In Proceedings of the 18th Australasian Fluid Mechanics

Conference (AFMC 2012). University of Southern Queensland.

[5] Al-Faruk, A. and Sharifian, A., 2016. Geometrical optimization of a swirling Savonius wind turbine using an open jet wind tunnel. Alexandria Engineering Journal, 55(3), pp.2055-2064.

[6] Al-Faruk, A. and Sharifian, A., 2017. Flow field and performance study of vertical axis Savonius type SST wind turbine. Energy Procedia, 110, pp.235-242.

[7] Al-Faruk, A. and Sharifian, A.S., 2015. Effects of flow parameters on the performance of vertical axis swirling type Savonius wind turbine. International Journal of Automotive & Mechanical Engineering, 12.

[8] Al-Faruk, A. and Sharifian, A., 2014, December. Influence of blade overlap and blade angle on the aerodynamic coefficients in vertical axis swirling type Savonius wind turbine. In 19th Australasian Fluid Mechanics Conference. Melbourne, Australia.

[9] Al-Faruk, A., Sharifian, S.A. and Al-Atresh, S., 2012. Numerical investigation of performance of a new type of Savonius turbine. In Proceedings of the 18th Australasian Fluid Mechanics Conference (AFMC 2012) (pp. 1-4). Australasian Fluid Mechanics Society.

[10] Sharifian, A., & Hashempour, J. (2016). A novel ember shower simulator for assessing performance of low porosity screens at high wind speeds against firebrand attacks. Journal of fire sciences, 34(4), 335-355.

[11] Sharifian, A., & Hashempour, J. (2020). Wind tunnel experiments on effects of woven wire screens and buffer zones in mitigating risks associated with firebrand showers. Australian Journal of Mechanical Engineering, 18(2), 156-168.

[12] Hashempour, J., & Sharifian, A. (2017). Effective factors on the performance of woven wire screens against leaf firebrand attacks. Journal of fire sciences, 35(4), 303-316.

[13] Sharifian Barforoush, A., & Du Preez, M. (2022). Quantifying the effectiveness of a mesh in mitigating burning capabilities of firebrand shower. Fire, 5(5), 150.

[14] Blocken, B., Stathopoulos, T., Carmeliet, J., & Hensen, J. L. (2011). Application of computational fluid dynamics in building performance simulation for the outdoor environment: an overview. Journal of building performance simulation, 4(2), 157-184.

[15] AirSmart. (2020). Venturi system effect. Cool Pro Air. https://coolproair.com.au/airsmart-venturi/

[16] Merksamer, I. (2015). Venturi Refrigeration System. (Australian Patent No. US20150135741A1). https://patents.google.com/patent/US20150135741A1/en

[17] Wen, M. Y., Lee, C. H., & Tasi, J. C. (2008). Improving two-phase refrigerant distribution in the manifold of the refrigeration system. Applied Thermal Engineering, 28(17-18), 2126-2135.

[18] Etminan, A., Harun, Z., & Sharifian, A. (2016). Numerical simulation of three dimensional

turbulent flow structure and heat transfer in ribbed-straight, divergent and convergent ducts. International Journal of Mechanics, 10, 362-367.

[19] Randall, L. N. (1952). Rocket applications of the cavitating Venturi. Journal of the American Rocket Society, 22(1), 28-38.

[20] Wagoner, G. W., & Livingston, A. E. (1928). Application of the venturi meter to measurement of blood flow in vessels. Journal of Pharmacology and Experimental Therapeutics, 32(3), 171-180.

[21] Ball, C. M., & Featherstone, P. J. (2016). The Lungmotor. Anaesthesia and Intensive Care, 44(2), 187-188.

[22] Ustinov, S. (2016). Features of selection of flow measurement methods and devices for flow measuring of liquefied petroleum gas in pipelines.

[23] Kaladgi, A. R., Mukhtar, A., Afzal, A., Kareemullah, M., & Ramis, M. K. (2020, July). Numerical Investigation of Beta Ratio and Reynolds Number Effect on Coefficient of Discharge of Venturimeter. In IOP Conference Series: Materials Science and Engineering (Vol. 884, No. 1, p. 012116). IOP Publishing.

[24] Reader-Harris, M. (2015). Orifice plates and venturi tubes (pp. 13-14). Basel, Switzerland:: Springer International Publishing.

[25] International Organization for Standardization. (2003). Measurement of fluid flow by means of pressure differential devices inserted in circular cross-section conduits running full — part 4: venturi tubes (ISO-5167-4:2003). https://www.iso.org/standard/30192.html#:~:text=ISO%205167%2D4%3A2003%20is,diameter%20ratio%20and%20Reynolds%20number.

[26] Adelaja, A. O., Dirker, J., & Meyer, J. P. (2015). Experimental investigation of frictional pressure drop in inclined tubes. International Conference on Heat Transfer, Fluid Mechanics and Thermodynamics.

[27] Hojati, S. A., & Hanafizadeh, P. (2014, July). Effect of inclination pipe angle on oil-water two phase flow patterns and pressure loss. In Engineering Systems Design and Analysis (Vol. 45844, p. V002T11A006). American Society of Mechanical Engineers.

[28] Demir, S. (2020). CFD analysis of mini venturi-type air flowmeters for lab-scale applications. Sigma Journal of Engineering and Natural Sciences, 38(2), 603-612.

[29] Sharp, Z. B., Johnson, M. C., & Barfuss, S. L. (2018). Optimizing the ASME Venturi recovery cone angle to minimize head loss. Journal of Hydraulic Engineering, 144(1), 04017057.

[30] Prasanna, M. A., Seshadri, V., & Kumar, Y. (2016). Numerical analysis of compressible effect in the flow metering by classical venturimeter. Int J Eng Sci Res Technol, 5, 603-616.

[31] Sleigh, P. A. (2009). Boundary layer theory. An Introduction To Fluid Mechanics: CIVE1400. http://www.sleigh-munoz.co.uk/fluidsnotes/FluidsLevel1/Unit04/T2.html

[32] Liu, P., Liu, H., Yang, Y., Wang, M., & Sun, Y. (2020). Comparison of design methods for negative pressure gradient rotary bodies: A CFD study. Plos one, 15(1), e0228186.

[33] Sparrow, E. M., Abraham, J. P., & Minkowycz, W. J. (2009). Flow separation in a diverging conical duct: Effect of Reynolds number and divergence angle. International Journal of Heat and Mass Transfer, 52(13-14), 3079-3083.

[34] Fried, E., & Idelchik, I. E. (2017). Flow resistance: a design guide for engineers. Routledge.

[35] White, F. M. (2008), Fluid Mechanics, 6th edn, McGraw Hill, Berlin.

[36] Walia, P. S. (1998). Influence of polymeric additives on the melting and crystallization behavior of nylon 6, 6. West Virginia University.

[37] Orr, G., & Roth, M. (2012). Safe and consistent method of spot-welding platinum thermocouple wires and foils for high temperature measurements. Review of scientific instruments, 83(8), 084901.

[38] Tu, J., Yeoh, G. H., & Liu, C. (2018). Computational fluid dynamics: a practical approach. Butterworth-Heinemann.

[39] Cantwell, B. J. (2019). A universal velocity profile for smooth wall pipe flow. Journal of Fluid Mechanics, 878, 834-874.

[40] Versteeg, H. K., & Malalasekera, W. (2007). An introduction to computational fluid dynamics: the finite volume method. Pearson education.

[41] Sherrard, R. (2020). ANSYS Fluent-Tips, Tricks, and Troubleshooting. https://support.nimbix.net/hc/en-us/articles/360044738671-ANSYS-Fluent-%20Tips-Tricks-and-Troubleshooting

[42] Fluent, ANSYS. (2013). ANSYS fluent theory guide 15.0. ANSYS, Canonsburg, PA, 33.

[43] Reader-Harris, M. J., Barton, N., Brunton, W. C., Gibson, J. J., Hodges, D., Nicholson, I. G., & Johnson, P. (2000, October). The discharge coefficient and through-life performance of Venturi tubes. In Proceedings of 18th North Sea Flow Meas Workshop, Gleneagles, paper (Vol. 5).

[44] Menon, E. S. (2009). Working Guide to Pump and Pumping Stations: Calculations and Simulations. Gulf Professional Publishing.